

1 **Revision 2**

2 **Hydrothermal synthesis and crystal structure of  $\text{AlSO}_4(\text{OH})$ :**

3 **A titanite-group member**

4  
5 **ALAN J. ANDERSON,<sup>1</sup> HEXIONG YANG,<sup>2\*</sup> AND ROBERT T. DOWNS<sup>2</sup>**

6  
7 <sup>1</sup>Department of Earth Sciences, St. Francis Xavier University, Antigonish, Nova Scotia, Canada,  
8 B2G 2W5

9 <sup>2</sup>Department of Geosciences, University of Arizona, Tucson, Arizona 85721-0077, U.S.A.

10 \*Corresponding author: [hyang@email.arizona.edu](mailto:hyang@email.arizona.edu)

11 **ABSTRACT**

12 Aluminum hydroxysulfate,  $\text{AlSO}_4(\text{OH})$ , is postulated to play a vital role in controlling the  
13 solubility of aluminum in sulfate-rich acidic soils and ground waters, but it has not yet been  
14 confirmed in nature. This study reports the synthesis of an  $\text{AlSO}_4(\text{OH})$  crystal at 700 °C and ~1.0  
15 GPa in a hydrothermal diamond anvil cell from a mixture of 95%  $\text{H}_2\text{SO}_4$  and  $\text{Al}_2\text{O}_3$  powder and  
16 its structure determination from single-crystal X-ray diffraction data.  $\text{AlSO}_4(\text{OH})$  is monoclinic  
17 with space group  $C2/c$  and unit-cell parameters  $a = 7.1110(4)$ ,  $b = 7.0311(5)$ ,  $c = 7.0088(4)$  Å,  $\beta$   
18  $= 119.281(2)^\circ$ , and  $V = 305.65(3)$  Å<sup>3</sup>. Its crystal structure is characterized by kinked chains of  
19 corner-sharing  $\text{AlO}_6$  octahedra that run parallel to the  $c$ -axis. These chains are linked together by  
20  $\text{SO}_4$  tetrahedra and hydrogen bonds, forming an octahedral-tetrahedral framework. Except for the  
21 numbers and positions of H atoms,  $\text{AlSO}_4(\text{OH})$  is isostructural with the kieselite-type minerals, a  
22 subgroup of the titanite group of minerals. A comparison of powder X-ray diffraction patterns  
23 indicates that our  $\text{AlSO}_4(\text{OH})$  is the same as that obtained by Shanks et al. (1981) through  
24 hydrolysis of  $\text{Al}_2(\text{SO}_4)_3$  solutions at temperatures above 310 °C. To date,  $\text{AlSO}_4(\text{OH})$  has been  
25 synthesized only at temperatures above 290 °C, implying that it may not be stable in low-  
26 temperature environments, such as acidic soils and mine waters. The possible environments to  
27 find  $\text{Al}(\text{OH})\text{SO}_4$  may include places where sulfur-rich magma-derived fluids react with  
28 aluminous rocks under elevated temperature and pressure, and on Venus where a sulfur-rich  
29 atmosphere interacts with surface rocks at temperatures above 400 °C.

30  
31 **Keywords:**  $\text{AlSO}_4(\text{OH})$ , aluminum hydroxysulfate, X-ray diffraction, crystal structure, Raman  
32 spectroscopy, high temperature.

33

## INTRODUCTION

34 Aluminum hydroxysulfates are of great importance as precursor materials for preparation  
35 of various activated aluminas, catalysts,  $\alpha$ -aluminas, and quality ceramic products (e.g.,  
36 Cornilsen and Reed 1979; Maczura et al. 1994). Of the many compounds in the system  $\text{Al}_2\text{O}_3$ -  
37  $\text{SO}_3$ - $\text{H}_2\text{O}$  (Basset and Goodwin 1949; Dyson and Scott 1965; Nordstrom 1982), only about a  
38 dozen are known to occur naturally in low-temperature environments, such as hydrobasaluminite  
39  $\text{Al}_4\text{SO}_4(\text{OH})_{10}\cdot 9\text{H}_2\text{O}$ , felsöbányaite  $\text{Al}_4\text{SO}_4(\text{OH})_{10}\cdot 4\text{H}_2\text{O}$ , alunogen  $\text{Al}_2(\text{SO}_4)_3(\text{H}_2\text{O})_{12}\cdot 5\text{H}_2\text{O}$ , and  
40 jurbanite/rostite  $\text{AlSO}_4(\text{OH})\cdot 5\text{H}_2\text{O}$ . Numerous studies have shown that some aluminum  
41 hydroxysulfates play a vital role in controlling the solubility of aluminum in sulfate-rich acidic  
42 soils and ground waters (e.g., Van Breemen 1976; Nordstrom 1982; Arp and Ouimet 1986;  
43 Bigham and Nordstrom 2000; Jones et al. 2011). In particular, based on the observations on  
44 aluminum activities in 127 acid mine waters and acid sulfate soil waters, Van Breemen (1973)  
45 found, for a wide range of pH, pAl, and pSO<sub>4</sub>, that there was a fairly constant proportion of  
46 Al:OH:SO<sub>4</sub> = 1:1:1, and suggested that a basic aluminum sulfate mineral of this stoichiometry  
47 controlled the dissolved aluminum concentrations. Further evidence to support this unknown  
48 mineral as a control on dissolved aluminum in acid sulfate soils and acid mine waters was  
49 provided by Van Breemen (1976) and Nordstrom (1982). Consequently, a new approach, called  
50 the  $\text{AlSO}_4(\text{OH})$  approach or a constant solubility product of  $\text{AlSO}_4(\text{OH})$  (Ludwig et al. 1999),  
51 has been proposed to model soil solution field data (Prenzel and Meiwes 1994; Ludwig et al.  
52 1999), as compared to the classical sorption isotherm approach (e.g., Alewell et al. 1995, 1997).  
53 Nevertheless, Van Breemen's conjectured mineral has not yet been discovered in nature,  
54 possibly because it may be very fine-grained and amorphous (Van Breemen 1973; Nordstrom  
55 1982). It should be pointed out that the compound  $\text{AlSO}_4(\text{OH})$  was also expressed as  $\text{Al}(\text{OH})\text{SO}_4$   
56 or  $\text{AlOHSO}_4$  in the literature. However, to facilitate a direct comparison with the kieserite-group  
57 minerals, we have adapted the formula  $\text{AlSO}_4(\text{OH})$  throughout this paper.

58 Several experiments at temperatures above 100 °C, however, have produced other  
59 aluminum hydroxysulfates by hydrolysis of  $\text{Al}_2(\text{SO}_4)_3$  solutions (Basset and Goodwin 1949;  
60 Dyson and Scott 1965; Shanks et al. 1981). Of special interest is "phase A" synthesized at 290  
61 °C by Dyson and Scott (1965). This new phase has the composition  $\text{AlSO}_4(\text{OH})$  and does not  
62 appear at much lower temperatures (for example, 250 °C). It dehydrates upon heating above 550  
63 °C. Shanks et al. (1981) obtained fine crystalline  $\text{AlSO}_4(\text{OH})$  from 127 and 336 g/l  $\text{Al}_2(\text{SO}_4)_3$

64 solutions at temperatures greater than 310 °C and suggested that the high-temperature hydrolysis  
65 product,  $\text{AlSO}_4(\text{OH})$ , could represent a possible state-of-the-art alternative to recovering alumina  
66 from  $\text{Al}_2(\text{SO}_4)_3$ . This study reports the first structure analysis of hydrothermally synthesized  
67  $\text{AlSO}_4(\text{OH})$  with single-crystal X-ray diffraction and Raman spectroscopy.

68

69

## EXPERIMENTAL METHODS

70 The  $\text{AlSO}_4(\text{OH})$  crystal used in this study was synthesized in a hydrothermal diamond  
71 anvil cell (HDAC) from a solution consisting of concentrated 95-98% sulfuric acid (*Alfa Aesar*  
72 CAS: 7664-93-9) and  $\text{Al}_2\text{O}_3$  powder (~35g/l). The solution with an air bubble was enclosed in a  
73 cylindrical-shaped sample chamber (300  $\mu\text{m}$  in diameter and 40  $\mu\text{m}$  in height) that was milled  
74 into one of the diamond anvils (Anderson et al. 2002). The fluid sample was examined using a  
75 petrographic microscope as it was heated at a rate of 10 °C / minute. The air bubble disappeared  
76 as the temperature reached 358 °C. At 700 °C, a single prismatic crystal measuring 80 × 20 × 15  
77  $\mu\text{m}$  precipitated from the solution (Fig. 1). The pressure in the HDAC at 700 °C was estimated to  
78 be ~1.0 GPa using an isochore constructed from the equation of state of  $\text{H}_2\text{O}$ . The crystal was  
79 extracted from the HDAC after cooling to room temperature.

80 Because only one  $\text{AlSO}_4(\text{OH})$  crystal was synthesized, we did not prepare it for the  
81 quantitative chemical measurement with electron microprobe analysis. A qualitative chemical  
82 analysis of the crystal was conducted on a Hitachi 3400N scanning electron microscope  
83 equipped with an Oxford EDS/EBSD system, revealing that Al, S and O are the major  
84 constituents, with trace Cr, which results most likely from the interaction of  $\text{H}_2\text{SO}_4$  with  
85 nichrome wire used for resistance heating in the HDAC.

86 Single-crystal X-ray diffraction data of  $\text{AlSO}_4(\text{OH})$  were collected on a Bruker X8  
87 APEX2 CCD X-ray diffractometer equipped with graphite-monochromatized  $\text{MoK}\alpha$  radiation  
88 and frame widths of 0.5° in  $\omega$  and 30 s counting time per frame. All reflections with  $I > 2\sigma(I)$   
89 were indexed based on a monoclinic unit cell (Table 1). No satellite or super-lattice reflections  
90 were observed. The intensity data were corrected for X-ray absorption using the Bruker program  
91 SADABS. The systematic absences of reflections suggest the possible space groups  $C2/c$  or  $Cc$ .  
92 The crystal structure was solved and refined using SHELX97 (Sheldrick 2008) based on the  
93 space group  $C2/c$ , because it yielded a better refinement statistics in terms of bond lengths and  
94 angles, atomic displacement parameters, and  $R$  factors. The positions of all atoms were refined

95 with anisotropic displacement parameters, except for the H atom, which was refined  
96 isotropically. During the structure refinements, an attempt to refine the site occupancy of  $\text{Al}^{3+}$  vs.  
97  $\text{Cr}^{3+}$  was made, showing no detectible Cr substitution for Al in the crystal. The ideal chemical  
98 formula,  $\text{AlSO}_4(\text{OH})$ , was thus assumed in the refinements. Final atomic coordinates and  
99 displacement parameters are listed in Table 2 and selected bond lengths and angles in Table 3.

100 The Raman spectrum of  $\text{AlSO}_4(\text{OH})$  was recorded from a random orientation on a  
101 Thermo Almega microRaman system, using a solid-state laser with a frequency of 532 nm and a  
102 thermoelectrically cooled CCD detector. The laser is partially polarized with  $4\text{ cm}^{-1}$  resolution  
103 and has a spot size of  $1\ \mu\text{m}$ .

104

## 105 RESULTS AND DISCUSSION

106 The crystal structure of  $\text{AlSO}_4(\text{OH})$  is characterized by kinked chains of corner-sharing  
107  $\text{AlO}_6$  octahedra that extend parallel to the *c*-axis. These chains are linked together by  $\text{SO}_4$   
108 tetrahedra and hydrogen bonds, forming an octahedral-tetrahedral framework (Fig. 2a). Except  
109 for the numbers and positions of H atoms,  $\text{AlSO}_4(\text{OH})$  is isostructural with the kieserite-type  
110 minerals,  $M^{2+}\text{SO}_4\cdot\text{H}_2\text{O}$ , where  $M = \text{Mg, Ni, Co, Fe, Mn, Zn}$  (Hawthorne et al. 1987; Wildner  
111 and Giester 1991) (Table 1, Fig. 2b), which have been further classified into the titanite group of  
112 minerals (Baur 1959; Hawthorne et al. 1987). The determination of the  $\text{AlSO}_4(\text{OH})$  structure has  
113 thus added a new subgroup to the titanite-type family. Nevertheless, there are some noticeable  
114 structural discrepancies between  $\text{AlSO}_4(\text{OH})$  and kieserite  $\text{MgSO}_4\cdot\text{H}_2\text{O}$ . The most notable are the  
115 hydrogen bonding schemes, owing to the substitution of OH for  $\text{H}_2\text{O}$  (Fig. 2). In  $\text{AlSO}_4(\text{OH})$ , the  
116 H atom forms a bifurcated hydrogen bond with two O1 atoms, whereas in kieserite, the two H  
117 atoms form two normal asymmetrical hydrogen bonds with two O2 atoms. Moreover, the  
118 relatively strongly-bonded and rigid  $\text{Al}^{3+}\text{O}_6$  octahedron in  $\text{AlSO}_4(\text{OH})$  is less distorted than the  
119  $M^{2+}\text{O}_6$  octahedron in any of the kieserite-group minerals, as measured by the octahedral angle  
120 variance and quadratic elongation indices (OAV and OQE) (Robinson et al. 1971). The OAV  
121 and OQE values are 2.41 and 1.001, respectively, for the  $\text{AlO}_6$  octahedron in  $\text{AlSO}_4(\text{OH})$ , but  
122 9.7-15.6 and 1.005-1.008 for the  $\text{MO}_6$  octahedron in the kieserite-group minerals.

123 Wildner and Giester (1991) noted a strong inverse correlation between the *M*-O3-*M*  
124 kinking angle within the octahedral chains in the kieserite-group minerals and the  $M^{2+}$  cation  
125 size. Our data on  $\text{AlSO}_4(\text{OH})$ , together with those for  $\text{FeSO}_4(\text{OH})$  (Ventruti et al. 2005), lend

126 further support to this observation (Fig. 3). However, there is an obvious discontinuity in the  
127 trend of the  $M$ -O3- $M$  angle vs. the cation size, suggesting that some abrupt structural changes  
128 take place with the coupled substitution of ( $M^{3+} + \text{OH}$ ) for ( $M^{2+} + \text{H}_2\text{O}$ ) in the kieserite-type  
129 structures. It thus follows that there may be an immiscibility gap between  $M^{3+}\text{SO}_4(\text{OH})$  and  $M$   
130  $^{2+}\text{SO}_4\cdot\text{H}_2\text{O}$ , due probably to the charge and size differences between  $M^{3+}$  and  $M^{2+}$ .

131 Shanks et al. (1981) reported a powder X-ray diffraction pattern for  $\text{AlSO}_4(\text{OH})$  obtained  
132 by the hydrolysis of  $\text{Al}_2(\text{SO}_4)_3$  solutions at temperatures above 310 °C. For comparison, we  
133 calculated the powder X-ray diffraction pattern for our  $\text{AlSO}_4(\text{OH})$  from the determined structure  
134 model using the program XPOW (Downs et al. 1993) (Fig. 4). The strong correlation of the two  
135 patterns indicates that the  $\text{AlSO}_4(\text{OH})$  obtained by Shanks et al. (1981) adopts the same crystal  
136 structure as ours.

137 Through the thermal decomposition of metahohmannite,  $\text{Fe}^{3+}_2\text{O}(\text{SO}_4)_2\cdot 4\text{H}_2\text{O}$ , Ventruti et  
138 al. (2005) obtained a compound with the composition  $\text{FeSO}_4(\text{OH})$  and measured its powder X-  
139 ray diffraction data at ~220 °C, which they claimed represents two distinct polymorphs. Phase 1,  
140 which is the same as that reported by Johansson (1962), is orthorhombic, with space group  $Pnma$   
141 and unit-cell parameters  $a = 7.33$ ,  $b = 6.42$ , and  $c = 7.14$  Å, whereas phase 2 is monoclinic, with  
142 space group  $P2_1/c$  and unit-cell parameters  $a = 7.33$ ,  $b = 7.14$ ,  $c = 7.39$  Å, and  $\beta = 119.7^\circ$ .  
143 However, an inspection of the phase-2 structure reveals that it is actually isostructural with our  
144  $\text{AlSO}_4(\text{OH})$ . Its true symmetry should be  $C2/c$ , rather than  $P2_1/c$ , with a transformation of their  
145 unit-cell parameters by the matrix  $[-1\ 0\ -1, 0\ 1\ 0, 1\ 0\ 0]$ . The transformed cell parameters for  
146  $\text{FeSO}_4(\text{OH})$  phase 2 are  $a = 7.394$ ,  $b = 7.14$ ,  $c = 7.33$  Å, and  $\beta = 119.75^\circ$ . Our conclusion has  
147 been validated by the PLATON program (Le Page 1987, 1988) and Prof. F. Scordari, the  
148 corresponding author for the work by Ventruti et al. (2005), agrees (personal communication).  
149 The transformed atomic coordinates for the phase-2 structure are listed in Table 2 for comparison  
150 with those for  $\text{AlSO}_4(\text{OH})$ . It is interesting to note that the similar compound  $\text{FeSO}_4(\text{OH})$   
151 exhibits two polymorphs, one being orthorhombic (Johansson 1962) and the other monoclinic  
152 (Ventruti et al. 2005).

153 The Raman spectrum of  $\text{AlSO}_4(\text{OH})$  is displayed in Figure 5. The major band  
154 assignments (Table 4) are based on previous spectroscopic studies of similar hydrous sulfates,  
155 including kieserite and alunite (e.g., Serna et al. 1986; Rudolph and Mason 2001; Lutz 2004;  
156 Frost et al. 2006; Kong et al. 2014). According to Libowitzky (1999), the O-H stretching band at

157 3549  $\text{cm}^{-1}$  corresponds to an estimated O...O distance of  $\sim 3.10 \text{ \AA}$ , which compares well with the  
158 O3...O1 distance ( $3.117 \text{ \AA}$ ) determined from the structure refinement (Table 3).

159 Until now,  $\text{AlSO}_4(\text{OH})$  has only been attained at temperatures above  $290 \text{ }^\circ\text{C}$  (Dyson and  
160 Scott 1965; Shanks et al. 1981; this study) and this is most likely one of the reasons why  
161  $\text{AlSO}_4(\text{OH})$  has not been found in low-temperature environments, such as surface soils and mine  
162 waters. A question remains regarding the identity of the enigmatic mineral with  $\text{Al}:\text{OH}:\text{SO}_4 =$   
163  $1:1:1$  that was postulated by Van Breemen (1973). From the solubility equilibrium calculations  
164 of aluminium sulfate minerals, Nordstrom (1982) found that the composition and solubility of  
165 Van Breemen's unknown mineral compares well with those of jurbanite/rostitite  
166  $\text{AlSO}_4(\text{OH})\cdot 5\text{H}_2\text{O}$ . In fact, except for  $\text{AlSO}_4(\text{OH})$ , jurbanite/rostitite is the only known aluminium  
167 hydroxysulfate having the ratio of  $\text{Al}:\text{OH}:\text{SO}_4 = 1:1:1$ . Yet, we cannot rule out the possible  
168 existence of a low-temperature polymorph of  $\text{AlSO}_4(\text{OH})$ , in addition to the  $C2/c$  form  
169 determined in this study.

170

171

## IMPLICATIONS

172 Newton and Manning (2005) suggested that a large proportion of solute sulfur in a mafic  
173 magma may partition into an exhalative saline fluid as sulfate. Given that sulfuric acid is an  
174 effective agent for removing aluminium from aluminous minerals, we suggest that the interaction  
175 of highly oxidized brines of juvenile/magmatic origin with aluminum-rich rocks could result in  
176 the formation of  $\text{AlSO}_4(\text{OH})$  at elevated pressure and temperature conditions in the Earth's crust.  
177 Another possible environment for  $\text{AlSO}_4(\text{OH})$  to occur is on the surface of Venus, where highly  
178 concentrated sulfuric acid in the atmosphere may interact with aluminum-bearing minerals on the  
179 surface at temperatures exceeding  $400 \text{ }^\circ\text{C}$ .

180 The method used for synthesis in this study may be further developed so that  
181 thermochemical measurements can be obtained. These data are requisite for understanding the  
182 stability of  $\text{AlSO}_4(\text{OH})$  in low-temperature environments and for predicting the occurrence of  
183  $\text{AlSO}_4(\text{OH})$  in the deep sulfur cycle.

184

185

## ACKNOWLEDGMENTS

186 A.J.A. acknowledges support from the GEN-IV program provided by Natural Resources  
187 Canada through the Office of Energy Research and Development, Atomic Energy of Canada

188 Limited, and Natural Sciences and Engineering Research Council of Canada. This work was also  
189 supported by the Science Foundation Arizona and NSF grant (EAR-0929777) for the University  
190 of Arizona SEM facility. The highly constructive communication with Prof. F. Scordari on the  
191 symmetry of the  $\text{FeSO}_4(\text{OH})$  phase is greatly appreciated.

192

## REFERENCES CITED

- 193 Alewell, C., Manderscheid, B., Lukewille, A., Koeppe, P., and Prensel, J. (1995) Describing soil  
194  $\text{SO}_4^{2-}$  dynamics in the Solling Roof Project with two different modelling approaches.  
195 Water, Air, and Soil Pollutions, 85, 1801-1806.
- 196 Alewell, C., Bredemeier, M., Matzner, E., and Blanck, K. (1997) Soil solution response to  
197 experimentally reduced acid deposition in a forest ecosystem. Journal of Environmental  
198 Quality, 26, 658-665.
- 199 Anderson, A.J., Jayanetti, S., Mayanovic, R.A., Bassett, W.A., and Chou, I-M. (2002) X-ray  
200 spectroscopic investigations of fluids in the hydrothermal diamond anvil cell: The  
201 hydration structure of  $\text{La}^{3+}$  from ambient to 300 °C and 1600 bars. American  
202 Mineralogist, 87, 262-268.
- 203 Arp, P.A., and Ouimet, R. (1986) Aluminum speciation in soil solutions: equilibrium  
204 calculations. Water, Air, and Soil Pollution, 31, 359-366.
- 205 Bassett, H., and Goodwin, T.H. (1949) The basic aluminum sulfates. Journal of the Chemical  
206 Society, 2239-2279.
- 207 Baur, W.H. (1959) Die Kristallstruktur des Edelamblygonits  $\text{LiAlPO}_4(\text{OH},\text{F})$ . Acta  
208 Crystallographica, 12, 988-994.
- 209 Bigham, J.M., and Nordstrom, D.K. (2000) Iron and aluminum hydroxysulfates from acid sulfate  
210 waters. In *Sulfate Minerals – Crystallography, Geochemistry and Environmental*  
211 *Significance*. Mineralogical Society of America, Washington DC, USA, pp. 351-403.
- 212 Cornilsen, B.C., and Reed, J.S. (1979) Homogeneous precipitation of basic aluminum salts as  
213 precursors for alumina. American Ceramic Society Bulletin, 58, 1199-1199.
- 214 Downs, R.T., Bartelmehs, K.L., Gibbs, G.V., and Boisen, M.B., Jr. (1993) Interactive software  
215 for calculating and displaying X-ray or neutron powder diffractometer patterns of  
216 crystalline materials. American Mineralogist, 78, 1104-1107.
- 217 Dyson, N.F., and Scott, T.R. (1965) New phases in the system  $\text{Al}_2\text{O}_3\text{-SO}_3\text{-H}_2\text{O}$  at temperatures  
218 above 100° C. Nature, 205, 358-359.
- 219 Frost, R., Wills, R-A., Weier, M., Martens, W., and Kloprogge, T. (2006) A Raman  
220 spectroscopic study of alunites. Journal of Molecular Structure, 785, 123-132.
- 221 Hawthorne, F.C., Groat, L.A., Raudsepp, M., and Ercit, T.S. (1987) Kieserite,  $\text{Mg}(\text{SO}_4)(\text{H}_2\text{O})$ , a  
222 titanite-group mineral. Neues Jahrbuch für Mineralogie, Abhandlungen, 157, 121-132.
- 223 Johansson, G. (1962) On the crystal structure of  $\text{FeOHSO}_4$  and  $\text{InOHSO}_4$ . Acta Chemica  
224 Scandinavica, 16, 1234-1244.
- 225 Jones, A.M., Collins, R.N., and Waite, D. (2011) Mineral species control of aluminum solubility  
226 in sulfate-rich acidic waters. Geochimica et Cosmochimica Acta, 75, 965-977.
- 227 Kong, W.G., Zheng, M.P., Kong, F.J. and Chen, W.X. (2014) Sulfate-bearing deposits at  
228 Dalangtan Playa and their implication for the formation and preservation of martian salts.  
229 American Mineralogist, 99, 283-290.
- 230 Le Page, Y. (1987) Computer derivation of the symmetry elements implied in a structure  
231 description. Journal of Applied Crystallography, 20, 264-269.



- 232 Le Page, Y. (1988) MISSYM1.1 - a flexible new release. *Journal of Applied Crystallography*,  
233 21, 983-984.
- 234 Libowitzky, E. (1999) Correlation of O-H stretching frequencies and O-H···O hydrogen bond  
235 lengths in minerals. *Monatshefte für Chemie*, 130, 1047-1059.
- 236 Ludwig, B., Khanna, P., and Prenzel, J. (1999) Some equilibrium approaches to study the  
237 retention and release of sulfate in some highly acid German subsoils. *Journal of*  
238 *Environmental Quality*, 28, 1327–1335.
- 239 Lutz, H.D. (2004) Crystal matrix and crystal double matrix spectroscopy. *Journal of Molecular*  
240 *Structure*, 704, 71–78.
- 241 Maczura, G., Moody, K., Anderson, E.M., and Kunka, M.K. (1994) Alumina. *American Ceramic*  
242 *Society Bulletin*, 73, 74-74.
- 243 Newton, R.C., and Manning, C.E. (2005) Solubility of anhydrite, CaSO<sub>4</sub>, in NaCl-H<sub>2</sub>O solutions  
244 at high temperatures and pressures: applications to fluid rock interactions. *Journal of*  
245 *Petrology*, 46, 701-716.
- 246 Nordstrom, D.K. (1982) The effect of sulfate on aluminum concentrations in natural waters:  
247 some stability relations in the system Al<sub>2</sub>O<sub>3</sub>-SO<sub>3</sub>-H<sub>2</sub>O at 298 K. *Geochimica et*  
248 *Cosmochimica Acta*, 46, 681-692.
- 249 Prenzel, J., and Meiwes, K.-J. (1994) Sulfate sorption in soils under acid deposition: Modeling  
250 field data from forest liming. *Journal of Environmental Quality*, 23, 1212–1217.
- 251 Robinson, K., Gibbs, G.V., and Ribbe, P.H. (1971) Quadratic Elongation: A Quantitative  
252 Measure of Distortion in Coordination Polyhedra. *Science*, 172, 567–570.
- 253 Rudolph, W.W., and Mason, R. (2001) Study of aqueous Al<sub>2</sub>(SO<sub>4</sub>)<sub>3</sub> solution under hydrothermal  
254 conditions: sulfate ion pairing, hydrolysis, and formation of hydronium alunite. *Journal of*  
255 *Solution Chemistry*, 30, 527-548.
- 256 Serna, C.J., Parda Cortina, C., and Garcia Ramos, J.V. (1986) Infrared and Raman study of  
257 alunite-jarosite compounds. *Spectrochimica Acta A, Molecular and Biomolecular*  
258 *Spectroscopy*, 42A, 729-734.
- 259 Shanks, D.E., Eisele, J.A., and Bauer, D.J. (1981) Recovery of aluminum hydroxyl sulfate from  
260 aluminum sulfate solution by high temperature hydrolysis. Volume 8550 of Report of  
261 investigations. U.S. Dept. of the Interior, Bureau of Mines. 10 p.
- 262 Sheldrick, G. M. (2008) A short history of *SHELX*. *Acta Crystallographica*, A64, 112-122.
- 263 Van Breeman, N. (1973) Dissolved aluminum in acid sulfate soils and in acid mine waters. *Soil*  
264 *Science Society of America Proceedings*, 37, 694-697.
- 265 Van Breeman, N. (1976) Genesis and solution chemistry of acid sulfate soils in Thailand.  
266 *Agriculture Research Reports*, 848, 263 pp. (Ph.D. Thesis).
- 267 Ventruti, G., Scordari, F., Schingaro, E., Gualtieri, A.F., and Meneghini, C. (2005) The order-  
268 disorder character of FeOH<sub>2</sub>SO<sub>4</sub> obtained from the thermal decomposition of  
269 metahohmannite, Fe<sup>3+</sup><sub>2</sub>(H<sub>2</sub>O)<sub>4</sub>[O(SO<sub>4</sub>)<sub>2</sub>]. *American Mineralogist*, 90, 679-686.

- 270 Wildner, M., and Giester, G. (1991) The crystal structures of kieserite-type compounds. I.  
271 Crystal structures of  $\text{Me(II)SO}_4 \cdot \text{H}_2\text{O}$  (Me=Mn,Fe,Co,Ni,Zn). Neues Jahrbuch für  
272 Mineralogie, Monatshefte, 1991, 296-306.

273 **Figure captions**

274 Figure 1. Secondary electron image of the  $\text{AlSO}_4(\text{OH})$  crystal mounted on a glass fiber with  
275 epoxy.

276 Figure 2. Crystal structures of (a)  $\text{AlSO}_4(\text{OH})$  and (b) Kieserite  $\text{MgSO}_4 \cdot \text{H}_2\text{O}$ . The small spheres  
277 represent the H atoms.

278 Figure 3. Variation of the  $M\text{-O-}M$  angle with the  $M$  cation size in the kieserite-type compounds.

279 Figure 4. Comparison of powder X-ray diffraction patterns of  $\text{AlSO}_4(\text{OH})$  obtained by the  
280 hydrolysis of the  $\text{Al}_2(\text{SO}_4)_3$  solutions at temperatures above  $310^\circ\text{C}$  (Shanks et al. 1981) and that  
281 by hydrothermal synthesis done in this study.

282 Figure 5. The Raman spectrum of  $\text{AlSO}_4(\text{OH})$ .

283

**TABLE 1.** Comparison of crystal data and refinement results for  $\text{AlSO}_4(\text{OH})$  and kieserite.

	Synthetic $\text{AlSO}_4(\text{OH})$	Kieserite
Ideal chemical formula	$\text{AlSO}_4(\text{OH})$	$\text{MgSO}_4 \cdot \text{H}_2\text{O}$
Crystal symmetry	Monoclinic	Monoclinic
Space group	$C2/c$	$C2/c$
$a(\text{\AA})$	7.1110(4)	6.981(2)
$b(\text{\AA})$	7.0311(5)	7.624(2)
$c(\text{\AA})$	7.0088(4)	7.645(2)
$\beta(^{\circ})$	119.281(2)	117.70(2)
$V(\text{\AA}^3)$	305.65(3)	355.6(2)
$Z$	4	4
$\rho_{\text{cal}}(\text{g}/\text{cm}^3)$	3.043	2.585
$\lambda(\text{\AA}, \text{MoK}\alpha)$	0.71073	0.7107
$\mu(\text{mm}^{-1})$	1.209	
$2\theta$ range for data collection	$\leq 65.18$	
No. of reflections collected	2037	
No. of independent reflections	556	598
No. of reflections with $I > 2\sigma(I)$	485	509 [ $I > 2.5\sigma(I)$ ]
No. of parameters refined	38	
R(int)	0.029	
Final $R_1, wR_2$ factors [ $I > 2\sigma(I)$ ]	0.025, 0.057	0.023 [ $I > 2.5\sigma(I)$ ]
Final $R_1, wR_2$ factors (all data)	0.031, 0.061	
Goodness-of-fit	1.051	
Reference	This study	Hawthorne et al. (1987)

284

285

**TABLE 2.** Coordinates and displacement parameters in atoms in  $\text{AlSO}_4(\text{OH})$  and  $\text{FeSO}_4(\text{OH})$  for comparison

Atom	<i>x</i>	<i>y</i>	<i>z</i>	$U_{\text{eq}}$	$U_{11}$	$U_{22}$	$U_{33}$	$U_{23}$	$U_{13}$	$U_{12}$
Al	0	1/2	0	0.0045(2)	0.0045(3)	0.0048(3)	0.0042(3)	-0.0001(2)	0.0021(2)	-0.0008(2)
*Fe1=Fe2	0	1/2	0							
S	0	0.12284(8)	1/4	0.0058(2)	0.0052(3)	0.0053(2)	0.0063(2)	0	0.0024(2)	0
*S	0	0.116	1/4							
O1	0.1878(2)	-0.0026(2)	0.3465(2)	0.0105(3)	0.0068(5)	0.0095(6)	0.0132(6)	0.0015(4)	0.0033(5)	0.0022(4)
*O1=O5	0.183	0	0.3415							
O2	0.0037(2)	0.2427(2)	0.0798(2)	0.0102(3)	0.0165(6)	0.0069(6)	0.0092(6)	0.0015(4)	0.0079(5)	-0.0002(4)
*O2=O3	0	0.23	0.084							
O3	0	0.5861(3)	1/4	0.0090(3)	0.0141(8)	0.0062(8)	0.0078(8)	0	0.0062(7)	0
*O4	0	0.60	1/4							
H	0	0.684(7)	1/4	0.042(1)						

287 \*: These data are for  $\text{FeSO}_4(\text{OH})$ , which were taken from Ventruri et al. (2005) after the transformation (see the text for discussion).

**TABLE 3.** Selected bond distances and angles in  $\text{AlSO}_4(\text{OH})$ 

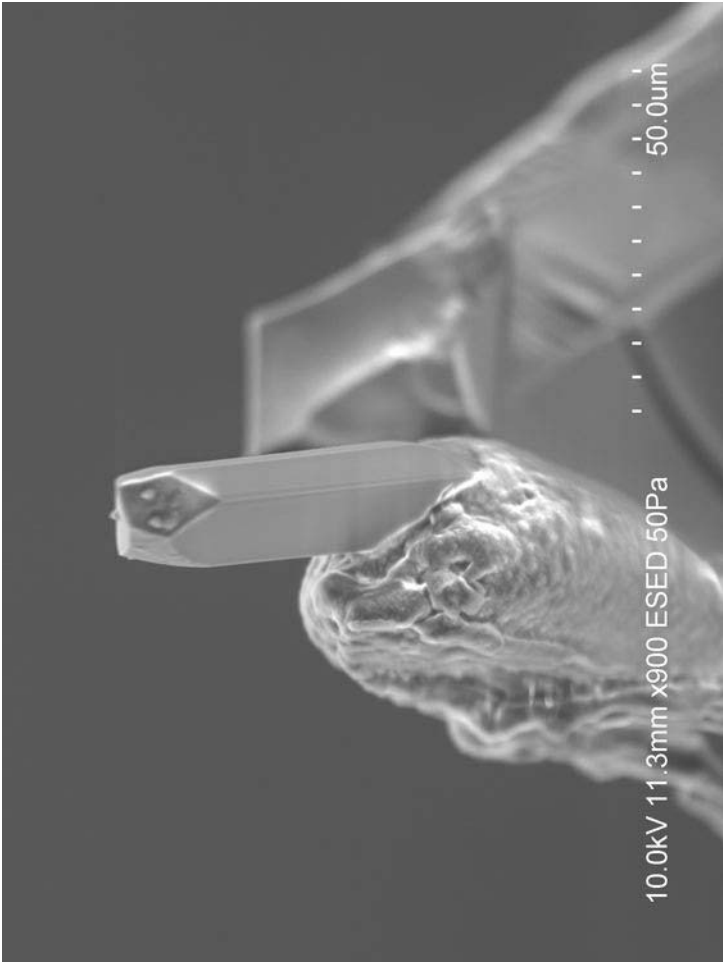
	Distance (Å)
Al—O1	1.937(1) x2
—O2	1.890(1) x2
—O3	1.854(1) x2
Avg.	1.894
OAV	2.413
OQE	1.001
S—O1	1.461(1) x2
—O2	1.472(1) x2
Avg.	1.466
TAV	3.352
TQE	1.001
O3—H	0.69(5)
O1...H	2.49(4)
O3...O1	3.117(2)
$\angle \text{O3—H...O1}$	152.1(5)°

Note: OAV = Octahedral angle variance; OQE = Octahedral quadratic elongation;

TAV = Tetrahedral angle variance; TQE = Tetrahedral quadratic elongation (Robinson et al. 1971).

**TABLE 4.** Tentative assignments of major Raman bands for  $\text{AlSO}_4(\text{OH})$ .

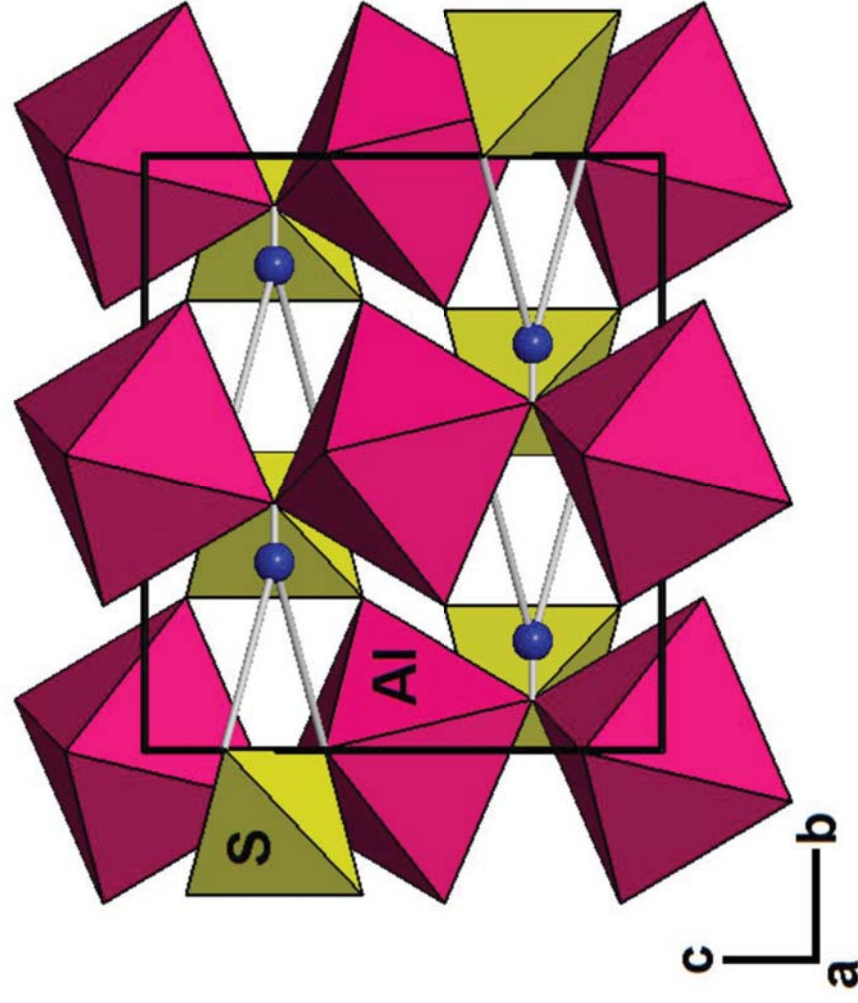
Bands ( $\text{cm}^{-1}$ )	Assignment
270	O-Al-O bending within $\text{AlO}_6$
405, 442	$\nu_2$ ( $\text{SO}_4$ ) symmetric bending
521	Al-O stretching within $\text{AlO}_6$
614, 670	$\nu_4$ ( $\text{SO}_4$ ) anti-symmetric bending
1102	$\nu_1$ ( $\text{SO}_4$ ) symmetric stretching
1148	$\nu_3$ ( $\text{SO}_4$ ) anti-symmetric stretching
3549	OH stretching



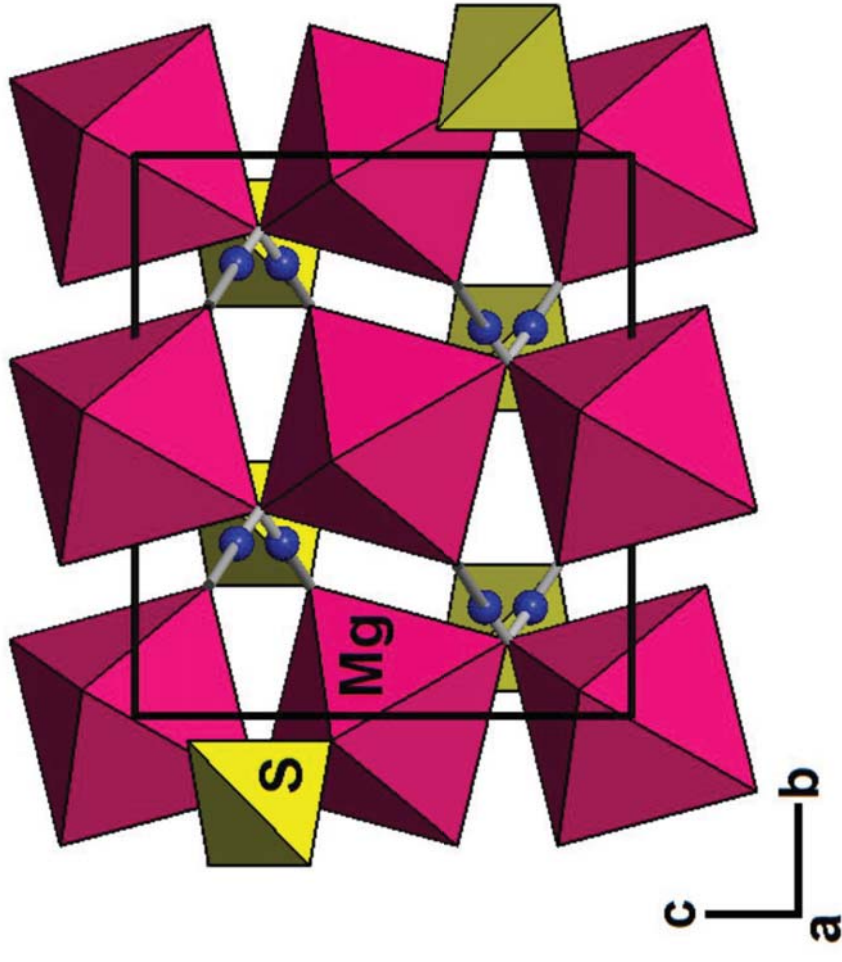
10.0kV 11.3mm x900 ESED 50Pa

50.0um





(a)  $\text{AlSO}_4(\text{OH})$



(b)  $\text{MgSO}_4 \cdot \text{H}_2\text{O}$  (kieserite)

